Civil Engineering Infrastructures Journal xx,xx

DOI: 10.22059/ceij.2026.400767.2369

Numerical Investigation of Shotcrete Retrofit for Enhancing the Blast Resistance of Reinforced Concrete Frames

#	Name	Email Address	Degree	Country	Affiliation
1	Shahidzadeh, Mohammad Sadegh	shahidzadeh@bkatu.ac.ir	Ph.D.	Iran	Assistant Professor, Department of Civil Engineering, Technical and Engineering Faculty, Behbahan Khatam Alanbia University of Technology, Behbahan, Iran
2	Karami, Ehsan	ekeksarasoft2018@gmail.com	MSc Student	Iran	Master's student in Civil-Structural Engineering, Technical and Engineering Faculty, Behbahan Khatam Alanbia University of Technology, Behbahan, Iran
3	Derakhshan Nezhad, Amir Hossein	amir.h.d.nezhad@semnan.ac.ir	MSc	Iran	M.Sc. in Civil Engineering – Structural Engineering, Department of Civil Engineering, Technical and Engineering Faculty, Behbahan Khatam Alanbia University of Technology, Behbahan, Iran

Received: 16/08/2025

Revised: 08/10/2025

Accepted: 31/12/2025

Abstract: Today, concrete buildings are resistant to fire, sound, and thermal pollution due to the availability of the required materials. Damping concrete buildings against dynamic forces is more than steel buildings. Therefore, by using appropriate retrofitting methods, these buildings

can be optimally used in construction. In this research, a 4-story observation tower structure with the dimensions of 5×65 floors with a reinforced concrete bending frame system in three seismic zones with design accelerations of 0.25, 0.3 and 0.35 at distances of 10 and 20 meters and under Blast loading with 100, 200, 300 and 400 kg of TNT with and without reinforcement with shotcrete was modeled, loaded and analyzed in ETABS and ABAQUS software. The results showed that reinforcing the frame with shotcrete reduces the displacement and energy input to it. In fact, the shotcrete layer like a protector, absorbs the destructive effects caused by the explosion and reduces the damage caused by the force of the explosion on the frame. Reinforcement with shotcrete increases the structure's resistance and the amount of damage and destruction of the frame against to reduce the blast load, also increasing the blast distance reduced the effect of increasing the explosive material and by reinforcing the frame, the effects of the blast load decreased with the increase of the explosive material compared to the case without reinforcement.

Keywords: Concrete Buildings, Observation Tower, Blast Loading, Shotcrete, ABAQUS

1. Introduction

In recent years, the safety of structures against blast loads has become a focal point for researchers due to the escalating terrorist threats, particularly for critical infrastructure such as border observation towers (Akhondi et al., 2021). The primary challenge facing the engineering community is developing robust tools for design under high-speed dynamic effects, where traditional analytical methods rely on simplifications due to the scarcity of experimental data (Ashteyat et al., 2025; Abebe and Mohammed, 2022). Numerical modeling is essential as a complement to physical experiments, although uncertainties in the nonlinear behavior of materials under high strain rates (such as spalling and strain-rate sensitivity) persist. The rise in terrorist incidents has heightened interest in passive defense strategies, which focus on resilient design without active countermeasures. Explosives are high-energy-density chemical compounds that generate a supersonic pressure wave (shock) through oxidation-reduction reactions (Aoude and Li, 2025; Badshah et al., 2021; Barazesh et al., 2024). This wave imparts peak pressures and impulses on the structure, which decay according to the scaled-distance law ($Z = R/W^{\{1/3\}}$) and result in short-duration impulsive loading (0.1–10 milliseconds), distinct from seismic loads (Hosseini and Hosseini, 2021). Nonlinear damage patterns are influenced by factors such as the type of explosive, standoff distance, material ductility, support geometry, and obstructions, often manifesting as local spalling, global displacement, or progressive collapse (Liu et al., 2021). Reinforced concrete (RC) frames exhibit inherently higher resistance to blasts compared to steel due to mass damping and confinement effects, but vulnerabilities stem from rebar ratios, concrete compressive strength (fc' > 30 MPa), and interaction with infill walls (Gao et al., 2024). Open-air explosions produce hemispherical waves with Friedlander decay, while confined explosions amplify reflections (Hao et al., 2025; Hou et al., 2022). Passive defense principles propose three levels of protection: high (superficial damage), medium (repairable damage with minimal casualties), and low (partial collapse with high risk). For observation towers critical for border surveillance structures must withstand both natural (seismic) and anthropogenic threats (IEDs up to 400 kg TNT

equivalent). Historical precedents, such as RC posts in Iraq, demonstrate the effectiveness of heavy RC mass in mitigating blast effects (Fan et al., 2021; Fathi et al., 2017). However, urban constraints often prevent increasing safe standoff distances, necessitating retrofit methods to enhance ductility without impairing functionality (Jahami et al., 2019). Explosives are standardized against 453 g TNT equivalents, and their effects can be mitigated through material upgrades (e.g., fibers for strain hardening) or energy-dissipating barriers. Recent research has advanced shotcrete retrofitting for blast resistance, utilizing high-velocity application (up to 100 m/s) to form bonded, fiber-reinforced layers that enhance confinement and reduce spalling (Wang, 2024; Karbaschi et al., 2017; Hou et al., 2022). For example, Akhondi et al. (2021) examined numerical models of masonry walls overlaid with shotcrete under out-of-plane blasts, reporting 40–60% reductions in mid-height displacements (tensile capacity ft > 3 MPa post-retrofit). Aoude and Li (2025) experimentally validated steel-fiber shotcrete layers on UHPC panels, attributing up to 70% reductions in rear-face displacements under 100 kg TNT at 3 m standoff to fiber bridging (Vf = 2%). Elbanna et al. (2023) demonstrated that 50 mm shotcrete overlays on RC columns increased axial capacity by 25% under close-in blasts (0.5 m), with finite element (FE) simulations confirming reduced shear cracking via dynamic triaxial confinement. While these studies are pivotal, they primarily target isolated components (walls, panels, columns) under idealized far-field blasts, often overlooking the coupled response of multi-story frames in seismic-prone areas where inherent seismic detailing (e.g., ductile detailing per ASCE 7-22) may synergistically enhance blast performance. Prior related research on explosion-seismic interactions includes Ozturk et al. (2010), who analytically investigated the seismic behavior of a historical monument in Turkey's Cappadocia region before and after retrofitting with CFRP sheets, demonstrating significant reductions in lateral displacement and improved seismic performance without damaging the historical fabric. Öztürk et al. (2010) evaluated the effect of seismic retrofitting with FRP on a historical monument in Niğde, Turkey, using numerical analyses, confirming effective improvements in seismic performance. Comparative analyses of RC structures under blast and seismic loads further highlight the need for integrated design approaches (Mustapha et al., 2025). Advances in fiber-reinforced concrete have shown promise in enhancing mechanical properties and blast resistance, including the use of polymer and glass fibers (Najimi et al., 2021; Fathi et al., 2017), steel fibers in ultra-high performance concrete (Gao et al., 2024; Xiao et al., 2024), and natural fibers like date palm to improve tensile strength (Mirzaie Aliabadi et al., 2025a). Moreover, machine learning techniques are emerging for predicting damage in RC slabs under blasts (Hao et al., 2025), while empirical modeling aids in understanding cyclic responses of RC columns (Ricci et al., 2023). Experimental and numerical studies on high-strength fiber-reinforced slabs under blasts provide insights into spall resistance and dynamic responses (Luccioni et al., 2018; Liu et al., 2021; Guo et al., 2024). Mechanical anisotropy in aligned fiber composites for 3D printing offers potential for customized retrofitting solutions (Ma et al., 2019), and numerical modeling of infilled masonry under blasts underscores the role of infills (Pandey and Bisht, 2016; Badshah et al., 2021; Barazesh et al., 2024; Yanget al., 2024). Deep neural networks can predict compressive strength in heavyweight concrete for blast-resistant applications (Hemati et al., 2025), and behavioral analysis of RC deep beams under dynamic loading

with varying strain rates supports strut-and-tie modeling (Salehi et al., 2025). In related material science advancements, numerical modeling of wave interactions with porous structures may inform blast wave propagation studies (Chen et al., 2024), while innovations in nanomaterials, such as phosphorus-enriched nanosheets for energy storage (Elbanna et al., 2023), cationic complexes for stable systems (Fan et al., 2021), and cathode materials for batteries (Li et al., 2023), could inspire next-generation additives for enhanced concrete durability. Regional factors, including climate and temperature, also influence material selection and marketing strategies for cement and plasticizers in blast-prone areas (Mirzaie Aliabadi et al., 2025b).

In this context, we examine the role of seismic design in blast resilience for Iranian border towers, assessing load-distance-material interactions and proposing safe standoffs (e.g., >15 m for 200 kg TNT) and retrofit requirements. This study uniquely bridges this gap by investigating shotcrete retrofitting for a full-scale 4-story RC moment-frame observation tower (square plan 5 m × 5 m with 5 m bay spacing, total height 65 m comprising 4 stories at 16.25 m each including 3.5 m floor-to-floor height plus slab/cover, atop a 4 m deep fixed foundation in stiff soil with shear wave velocity Vs > 760 m/s, Site Class C), seismically designed per Iranian Standard 2800 (accelerations 0.25–0.35g), under scaled air-blasts (100–400 kg TNT at 10–20 m standoff). Unlike component-level analyses, coupled ETABS-ABAQUS modeling is employed to assess holistic frame responses displacements, energy absorption, and damage indices revealing how seismic provisions amplify retrofit efficacy (e.g., 50–65% displacement reductions). By bridging seismic-blast synergies in high-risk contexts like Iran's borders, this work advances passive defense for vulnerable infrastructure, providing retrofit guidelines for similar towers where terrorist threats intersect seismic zones.

2. Explosion

An explosion refers to a rapid oxidation-reduction reaction that is accompanied by the formation of a large volume of hot gases. Explosives cause energy waves and damage to surrounding structures by rapidly releasing energy and compressing air molecules. The pressure intensity of these waves decreases with increasing distance and time. Depending on the location of the explosives and the type of their load on the structure, explosions are divided into three types: space, air, and surface explosions (Ashteyat et al., 2025). Improving the level of protection of people's lives and controlling the performance of the structure against the loads caused by the explosion is one of the factors that caused the construction of safe structures to be included in the instructions of designers and builders of structures. This type of reinforcement is considered a subset of passive defense, which refers to a set of sensitive measures requiring the use of military and civilian forces that prevent human casualties or minimize the amount of losses and casualties. One of the basic principles in passive defense is the creation of strong fortifications and structures, which play a very important role in maintaining facilities, equipment, manpower, and important and sensitive centers when faced with threats. Records of recent wars show that enemy attacks are not limited to military bases, and attacks on civilians have also taken place in cities and residential areas (Guo et al., 2024). On the other hand, by using different sciences and techniques in wars, it is necessary to have a plan and special strategies to deal with them. Considering the current and future threats, it is important to build a safe and resistant environment against the various effects of conventional weapons, such as blast

waves and the resulting forces. A structure may face various threats during its useful life. The threat must be described in such a way that it can be used in determining the vulnerability of the property by determining protective measures; that is, an understandable and articulate description of the threat must be reached, which can be used to express and describe the threat with quantitative and qualitative indicators. Threats and damages are divided into two categories based on their origin:

1- Threats caused by natural factors; We can mention natural disasters such as earthquakes, floods, storms, fires, snow, and ice, etc., in which human factors do not play a role. Most of these types of threats are considered by designers in the design process, and their effects and the forces applied to the structure by these types of threats are also considered in the design process.

2- Threats that are caused by human factors. An explosion can be called one of the most important human threats; unfortunately, in most cases, this type of threat is not taken into account in the design, which can lead to harmful effects.

Explosive pressures near the target are very intense and destructive, and by moving away from it, the intensity of the explosion and its destructive effects are reduced. A simple solution can be considered for this threat, and that is to increase the explosion distance from the bomb. But this is not possible in most cases due to various reasons, including architectural and urban restrictions, and it is necessary to make the structure resistant to explosion.

In general, there are three levels of protection for bombs: high, medium, and low. The main difference between the levels is the amount of damage allowed to buildings and property.

High level of protection: the building suffers superficial damage, and only superficial damage is inflicted on residents and property.

Medium level of protection: the building suffers severe damage, but the building is usable and there is little damage to the residents and property.

Low level of protection: the building suffers a lot of damage but collapses. Maybe repairing the building in this case is not economically viable; the possibility of damage to the building and residents is high (Elbanna et al., 2023).

As mentioned, it is necessary to pay attention to the issue of passive defense. Our country, Iran, due to its special position in the Middle East and the world, due to the provision of energy resources, is always at risk of terrorist attacks, and special attention should be paid to this issue. Failure to take into account the strengthening of structures against explosion may cause irreparable damage. Therefore, the retrofitting of the Bani Observatory building should be evaluated and done using the latest advances in the construction industry. An explosion occurs when a large amount of energy in the form of heat and pressure is released quickly and suddenly. Explosive loading characteristics are generally influenced by the source and behavior of the explosive. The general characteristics of the explosive substance are determined by using factors such as the amount of energy, energy density, speed of energy release, and the power of the explosive substance. When the explosive material is ideal from the energy density and power of its source, the explosion can be described using one factor, the amount of total energy.

3. Shotcrete

Concrete spraying, also known as shotcrete, refers to the process of applying concrete or mortar at high velocity onto a structure or surface using compressed air. In this method,

a concrete mixture consisting of cement, sand, and aggregate is projected as a self-supporting, dense layer. The high velocity of shotcrete induces dynamic compression of the concrete, enhancing its structural performance. Shotcrete is a highly effective, reliable, and economical tool for ground control, applicable in the restoration and reconstruction of concrete structures and old buildings, primary maintenance in tunneling, stabilization of stone and soil slopes, and support of underground structures (Hou et al., 2022). Additionally, shotcrete can be defined as mortar or concrete sprayed onto a surface at high speed using compressed air. It is ideal for earth retention in tunneling and mining, providing rapid support after blasting and excavation, with suitable early strength that accommodates ground movement. The advantages of shotcrete include minimal or no need for formwork compared to other maintenance methods, suitability for irregular surfaces, and the ability to transport materials to hard-to-access locations. The primary goal of shotcrete application is to produce a final product with high strength and low permeability. One of the key characteristics of concrete is its high plasticity, and shotcrete is one of the most effective solutions to leverage this property. Shotcrete is employed for repairing existing structures and in applications that do not require formwork or involve complex, thin shapes. It is commonly used for the inner lining of tunnels, tanks, and prestressed concrete tanks, as well as for stabilizing steep rocky cliffs and covering steel plates to create fire-resistant shields.

Sprayed concrete has gained increasing importance in engineering construction in recent years. A critical characteristic of sprayed concrete is minimizing the rebound of concrete from the surface onto which it is applied. High adhesion, achieved through the use of thickening materials, significantly reduces rebound. Thick layers of sprayed repair mortar without concrete accelerators or antifreeze additives may experience spalling on vertical surfaces. This issue can be mitigated by using fiber-reinforced shotcrete with fine fibers; however, incorporating additional thickening materials can further address this problem (Ma et al., 2019). As an alternative to traditional shotcrete, macrosynthetic fibers can be used to enhance performance.

The advantages of the shotcrete process are as follows:

1) Increasing the spraying output up to 25 cubic meters per hour

2) Reducing the return mode by two to four times

3) Significant improvement of conditions in the work environment due to less dust production

4) Reducing costs related to corrosion in related equipment

5) Needs less air during spraying

6) Higher quality shotcrete (with constant water content)

3.1. Description of shotcrete execution method in concrete wall strengthening

First, the network of horizontal and vertical rebars is installed on the wall, and a layer of reinforced concrete is sprayed on the rebar network by shotcrete. This method includes the following steps:

1) Installing a network of horizontal and vertical rebars and connecting it to the existing wall with sewing reinforcements

2) The operation of spraying concrete with a certain thickness on the surface of the rebar network (shotcrete)

4. Validation

In order to validate the analysis performed in this research, the research of Wang et al. (2024) was used. The geometry of the model is according to Figure 1.

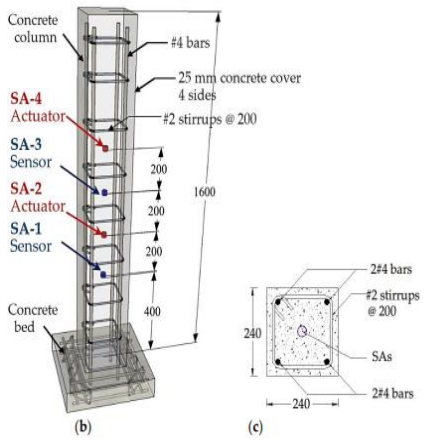

Fig. 1. Geometry and specifications of the model

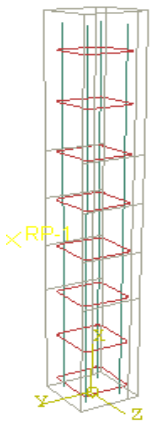

Fig. 2. Simulated column in Abaqus

All the members in the modeling were simulated completely according to the geometry of the model in the Abaqus software, and each of the sections was assigned to the desired member along with the specifications of the materials.

4.1. Modeling

Abaqus simulator program has been used for modeling, and this model was modeled in three dimensions. Table 1 and Figure 2 show the specifications of the desired column.

Table 1. Example of model B3 considered for modeling in the software

Description	Distance (cm)	Amount of mass (TNT) (g)	Test
Healthy condition	-	-	B_0
Explosion 1	50	40	B_1
Explosion 2	40	40	B_2
Explosion 3	30	40	B_3
Explosion 4	20	40	B_4
Explosion 5	0	40	B_5

4.2. Meshing

After transferring the model to the Mesh module in ABAQUS software, they are used to generate the elements and create the finite element model. Using the tools available in the mesh module of the Abaqus software, according to the data that is selected and meshed to solve the problem (according to Figure 3).

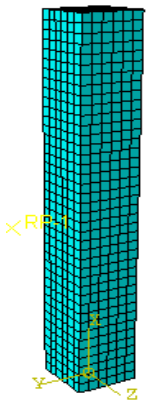

Fig. 3. Meshed model in ABAQUS

4.3. Loading and creation of boundary conditions

The loading and support conditions of the model are such that the support of the model is placed in the form of a girder and a column from a distance of 20 meters under the blast load superficially by the Canopy method (according to Figures 4 and 5).

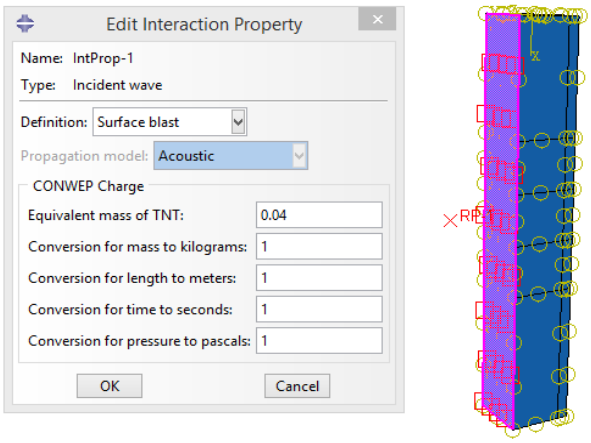

Fig. 4. Assigning the explosion load to a weight of 40 grams at a distance of 20 cm from the column

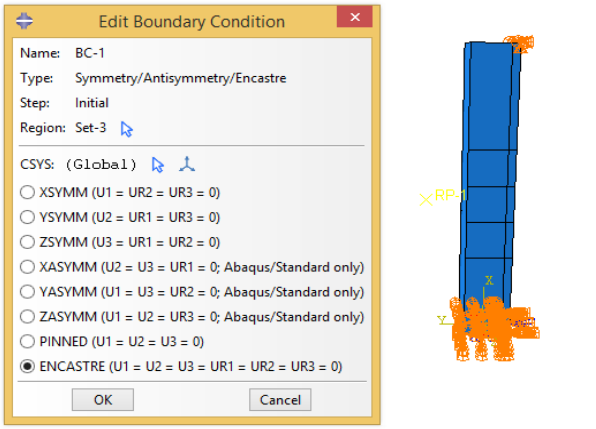

Fig. 5. Assigning the girder support to the model

In the Abaqus model, we have considered the boundary conditions according to the conditions of the article.

4.4. Model analysis

After completing all the modeling steps, it is time to analyze the model and obtain the intended outputs.

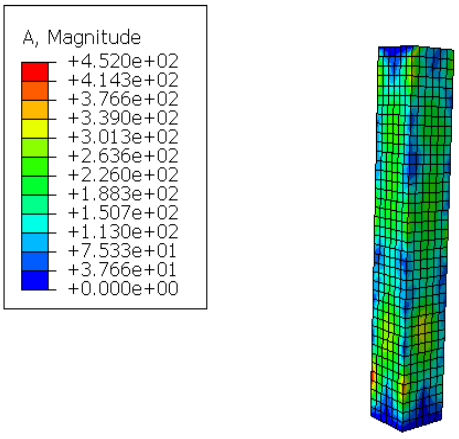

Fig. 6. Model analyzed in ABAQUS

4.5. Extracting ABAQUS outputs

After the analysis of the model, the acceleration-time diagram was extracted from the Visualization section, and the comparison of the acceleration-time diagram of the model designed with Abaqus software and Wang's research was done and presented according to Figures 7 and 8.

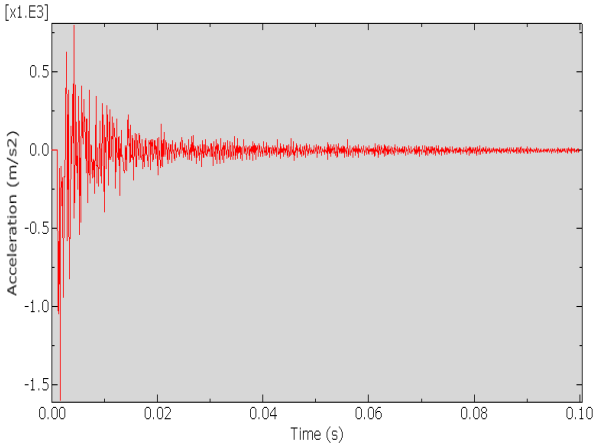

Fig. 7. Acceleration-time diagram obtained from Abaqus software

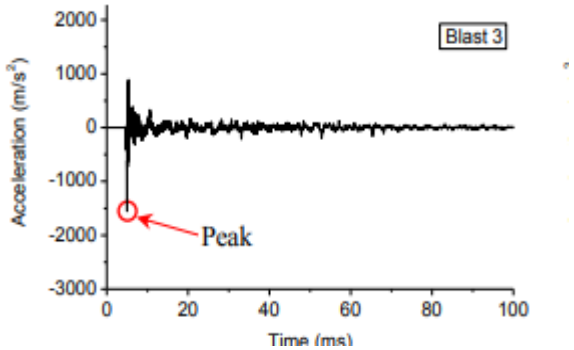

Fig. 8. Wang's acceleration-time diagram for the B3 model

After comparing the two acceleration-time graphs obtained from Abaqus and Wang's research, the difference percentage was obtained according to Table 2.

Table 2. Comparing the results of Wang's model and Abaqus software

Difference percentage of Wang and the numerical model	The difference between Wang's model and the numerical model (m/s^2)	Abaqus model acceleration (m/s^2)	Acceleration of Wang's research model (m/s^2)
5%	85	1585	1500

5. Modeling method

In this research, a 4-story observation tower structure with dimensions of 5×65 meters, featuring a reinforced concrete bending frame system, was modeled, loaded, and analyzed in ETABS software across three seismic zones with design accelerations of 0.25g, 0.30g, and 0.35g, according to the Iranian seismic design standard (Luccioni et al., 2018). The outputs of the analysis were extracted in the form of detailed beam, column, and rebar designs. Subsequently, leveraging the symmetry of the structure, one of the reinforced concrete frames was analyzed in the ABAQUS finite element software under blast loads with explosive charges of 100, 200, 300, and 400 kg of TNT at distances of 10 and 20 meters. The software outputs were evaluated in terms of displacement and absorbed energy.

5.1. Construction of model geometry (Part module)

In the Part module of ABAQUS/CAE, the geometry of a four-story reinforced concrete (RC) observation tower with a square plan (5×5 meters) and a total height of 65 meters was modeled in accordance with the Iranian National Building Code (INBC) Topic 6 and Standard 2800. The model represents a typical seismically designed border surveillance structure with enhanced blast resistance. The structural system consists of perimeter moment-resisting frames without shear walls, using 40×40 cm columns and 30×50 cm beams. Beams and columns were modeled using C3D8R solid elements, and reinforcing bars were defined using T_3D_2 truss elements. The interaction between rebars and concrete was modeled using the Embedded Region technique, assuming perfect bond behavior based on fib Model Code 2010. A mesh size ranging from 5 cm (near the blast face) to 20 cm elsewhere was adopted to balance computational efficiency and accuracy. Non-structural infill walls, constructed from 5 cm thick clay bricks with M5 mortar, were modeled as an equivalent orthotropic continuum (E_{eq} = 3.98 GPa, ν_{xy} = 0.15) using the Concrete Damaged Plasticity (CDP) model with tensile fracture energy G_f = 0.1 N/mm. This approach yielded less than 3% error in modal frequencies compared to detailed heterogeneous models. For blast retrofitting, galvanized steel mesh (10×10 cm, Φ4 mm, f_y = 250 MPa) was anchored to columns using Φ12 bolts (20 cm length) and overlaid with a 5 cm layer of fiber-reinforced shotcrete ($f'c$ = 35 MPa, V_f = 1% polypropylene fibers). The mesh was modeled using S4R shell elements and shotcrete with C3D8R solid elements. The interaction between the frame and infill was simulated

using nonlinear gap elements at the corners (kn = 100 kN/m, α = 0.15, per FEMA 356). This retrofitting system improves blast energy absorption (reducing rear-face velocities by 40–60% per UFC 3-340-02) without overloading the RC frame. Finally, by applying quarter-symmetry and anti-symmetric boundary conditions, the model's degrees of freedom were reduced by 75% while maintaining accuracy (less than 1% error in roof displacement). Material behavior was defined using nonlinear CDP for concrete and masonry, and J2 plasticity for steel and shotcrete, with strain-rate enhancement (DIF = 1.2 at strain rate $\dot{\varepsilon} = 10^2\ s^{-1}$). (according to Figure 9).

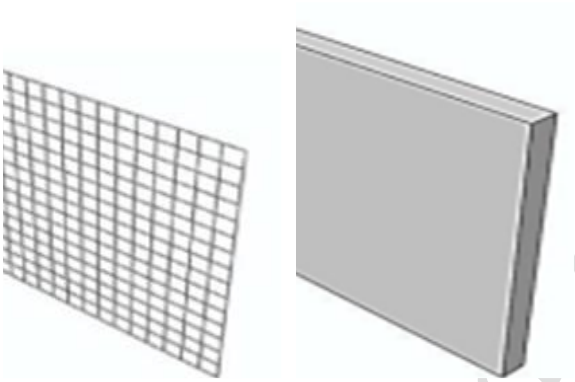

Fig. 9. 5 cm thick brick wall and 10 × 10 cm metal mesh

Considering the use of mortar between the bricks, the assumption of the homogeneity of the brick wall is far from reality; but for the ease of calculations, a homogeneous equivalent cross-section can be considered for the combination of brick wall and cover concrete. Due to the three-dimensional behavior of the wall and the translational degrees of freedom of the wall points, three-dimensional geometry is used to model the wall using the finite element method. For the steel mesh, due to the fact that the steel only transmits tension and pressure and has the same behavior as the truss members, three-dimensional mesh is used (according to Figures 10 and 11).

Fig. 10. Final modeling of non-reinforced frame model in Abaqus software

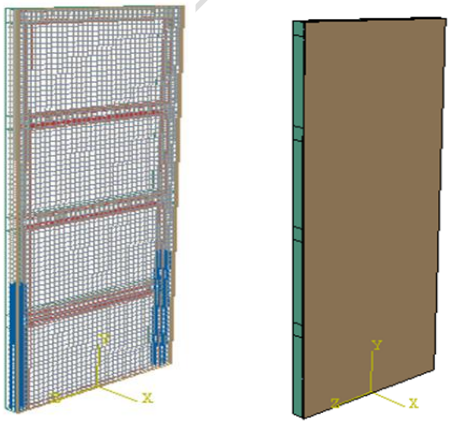

Fig. 11. The final modeling of the reinforced frame model with shotcrete in ABAQUS software

5.2. Specifications of materials

All material properties were defined and calibrated for nonlinear explicit dynamic analysis in ABAQUS using appropriate constitutive models. The Concrete Damaged Plasticity (CDP) model was employed for all cementitious components including concrete, shotcrete, and masonry. For steel materials, J2 isotropic hardening plasticity was adopted. To account for high strain-rate effects typical of blast loading conditions ($\dot{\varepsilon} \approx 10^2$–$10^3\ s^{-1}$), Dynamic Increase Factors (DIFs) were incorporated based on the recommendations of Malvar and Crawford (1998). Model

calibration was validated against experimental benchmarks:

Concrete and steel were calibrated based on uniaxial compression and tension tests, with stress-strain curve deviations kept below 8%, following the fib Model Code 2010. Masonry properties were validated using prism compression tests in accordance with ASTM C1314, with compressive strength deviations under 10%, referenced from. Material densities (ρ), elastic modulus (E), and Poisson's ratios (ν) represent quasi-static baseline values, while DIFs were applied as dynamic multipliers. For instance, $DIF_t = 1.2$ for tensile strength and $DIF_c = 1.05$ for compressive strength in concrete.

- **Concrete**

Compressive Strength: f′c = 30 MPa

Density: ρ = 2400 kg/m³

Elastic Modulus: E = 25.3 GPa

Poisson's Ratio: ν = 0.2

CDP Parameters:

Dilation angle (ψ) = 10°

Eccentricity (e) = 0.1

Biaxial-to-uniaxial compressive strength ratio (fb/fc) = 1.16

Flow potential shape factor (K) = 0.67

Viscosity (μ) = 0.001

Compressive Response:

Initial yield: $\sigma c_0/f'c = 1.16$

Damage parameter: dc = 0.85 at $\varepsilon c^{pl} = 0.0035$

Tensile Response:

Tensile strength: $ft_0 = 2.8$ MPa

Fracture energy: Gf = 0.1 N/mm

- **Shotcrete**

Shotcrete properties were modeled similar to concrete but with improved ductility.

Compressive Strength (post-curing): f′c = 35 MPa

Mix designs were rebound-adjusted and validated per ACI 506R-16.

- **Steel**

Yield Strength: fy = 300 MPa

Density: ρ = 7830 kg/m³

Elastic Modulus: E = 210 GPa

Poisson's Ratio: ν = 0.3

Plasticity Model: Isotropic hardening with multilinear stress–plastic strain relationship; kinematic hardening was neglected due to monotonic blast pulse conditions.

Dynamic Increase Factor: $DIF_s = 1.1$ for $\dot{\varepsilon} > 10\ s^{-1}$

Plastic stress–strain behavior is summarized in Table 3, calibrated against AISC 360-16 coupon tests (deviation <5% in ultimate strain).

Table 3. Plastic Stress–Strain Behavior of Steel

Plastic Strain	Yield Stress (Pa)
0.000	300,000,000
0.025	350,000,000
0.137	500,000,000
0.239	400,000,000
0.354	400,000,000

Masonry (Brick and Mortar Composite)

Homogenized properties were applied for infill walls, with experimental validation using prism compression and diagonal shear tests.

Density: ρ = 1830 kg/m³

Elastic Modulus: E = 3.98 GPa

Poisson's Ratio: ν = 0.15

Compressive Strength: fm = 10 MPa (per EN 1996-1-1)

CDP Parameters (Orthotropic Masonry):

Dilation angle (ψ) = 10°

Eccentricity (e) = 0.1

fb/fc = 1.16

Flow potential factor (K) = 0.67

Viscosity (μ) = 0.001

Shear Retention (post-cracking): β = 0.1

Stress–Strain Parameters:

Compressive:

Initial yield: $\sigma c_0/fm = 1.0$

Damage: dc = 0.9 at $\varepsilon c^{pl} = 0.002$

Tensile (Bed Joint):

$ft_0 = 0.2$ MPa

Fracture energy: Gf = 0.05 N/mm

Tables 4 and 5 provide detailed inelastic properties, corrected for unit consistency in Pascal.

Table 4. CDP Parameters for Masonry

Viscosity (μ)	K	fb/fc	Eccentricity (e)	Dilation Angle (ψ)
0.001	0.67	1.16	0.1	10°

Table 5. Compressive Inelastic Stress–Strain for Masonry

Inelastic Strain	Yield Stress (Pa)
0	12246667
0.0001	13048750
0.0002	13817230
0.0003	14552090
0.0005	15920980
0.0006	16555000
0.0007	17155420
0.0008	17722230
0.0009	18255420
0.001	18755000

These properties ensure accurate simulation of structural performance under blast loading. Masonry is modeled to exhibit brittle tensile failure (orthogonal cracking) and ductile compressive response. Global frame damage indices, such as Park–Ang (target <0.4), were controlled through material calibration. Sensitivity analyses confirmed that a ±10% variation in E led to <5% variation in peak displacements, indicating robustness of the defined material models.

5.3. Definition of the Step module as a problem-solving method and selecting desired outputs (Step module)

In the Step module, the type of analysis or analyses used in the research can be performed by Abaqus analysts in the form of the step definition. In fact, each single analysis is done in the form of a step. In the step, the initial conditions of the problem should be defined, such as initial temperature, initial velocity, or initial stresses if they are non-zero. In this part, the type of analysis for simulation is nonlinear dynamic, which is more suitable than the explicit solver due to the large number of model elements and the high volume of calculations that have complexity.

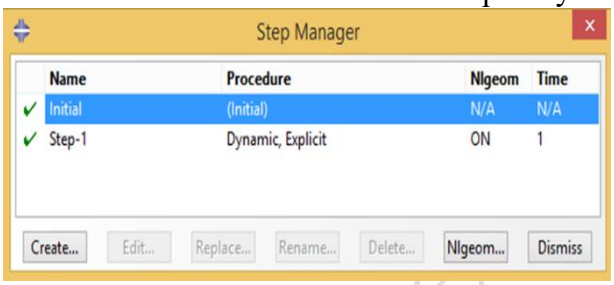

Fig.12. Defined steps for dynamic analysis

5.4. Definition of loading specifications and support conditions (load)

To model the explosion in the Step module, the Time Period value is taken into account in proportion to the duration of the explosion and the time required to better observe the effect of the explosion after loading calculations. To model the explosion, choose CONWEP and Air blast, and the amount of explosives is in kilograms and TNT, and in the next part, we will enter the explosion load and support conditions (according to Figures 13 and 14 and Table 6).

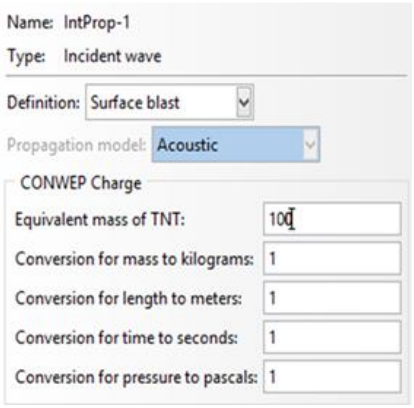

Fig.13. CONWEP Charge Definition for Incident Wave Simulation of 100 kg TNT Surface Blast

Table 6. Equivalent mass of explosion, distance, and time from the Interaction module

TNT equivalent mass	Seconds	m
100	0.01	10
200	0.01	10
300	0.01	10
400	0.01	10
100	0.01	20

200	0.01	20
300	0.01	20
400	0.01	20

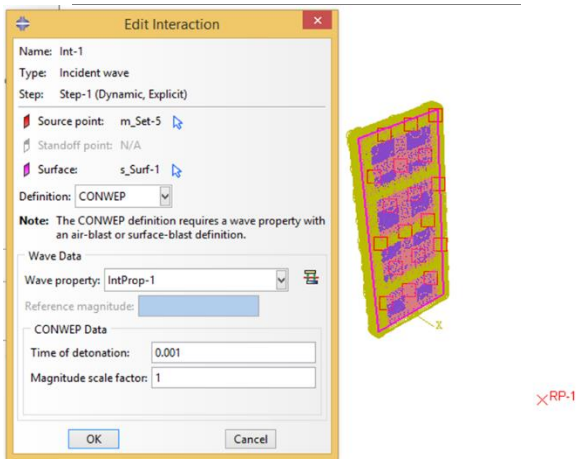

Fig. 14. Definition of Surface Blast Interaction Using CONWEP for 100 kg TNT Equivalent Load

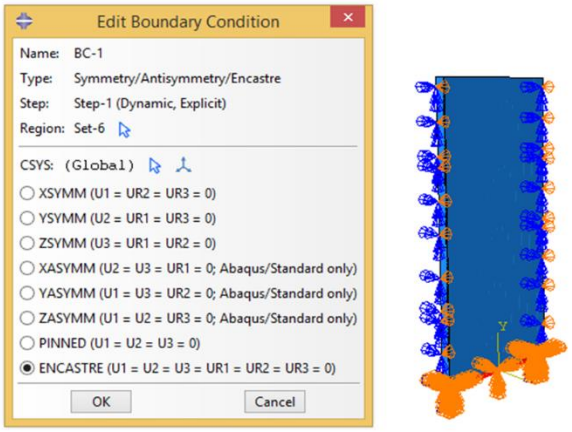

Fig. 15. Assignment of Symmetry/Antisymmetry Boundary Conditions in ABAQUS for Quarter-Model Simulation

5.5. Principles of model meshing

After transferring the model to the Mesh module in ABAQUS software, they are used to generate the elements and create the finite element model. Using the tools available in the mesh module of the Abaqus software, according to the solver chosen to solve the problem, the modeled structure is divided into smaller elements to analyze the section forces, which is called meshing. Every part or part in the part that has geometry (CAD geometry) needs to be meshed. In general, the meshing process consists of three steps. In the first step, the characteristics of each area, such as the type of elements, geometrical properties and materials used, are determined, and in the next step, the type and size of the elements are determined. At the end of the work, the geometry of the structure is meshed using suitable algorithms. The general rule in setting the finite element model is that the presence of extreme gradients in the used elements reduces the accuracy of the analysis. In the explicit solver method, the convergence is dependent on the length of the first time interval and the length of the elements as it follows a time step. The time step for solving the problem depends on the length of the element (each mesh unit) and its material (elasticity and volumetric mass); Therefore, the smaller the dimension of the defined mesh, the smaller the time step to solve the problem, and the total time to solve the problem increases. For this purpose, it is necessary to mesh the elements in such a way that both the objectives of the analysis are satisfied and the time cost of the analysis is optimal.

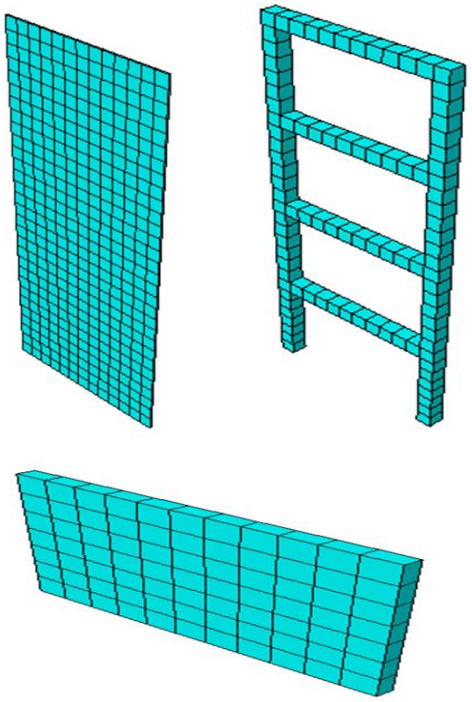

Fig. 16. Meshing of the frame model between the frame and the shotcrete wall

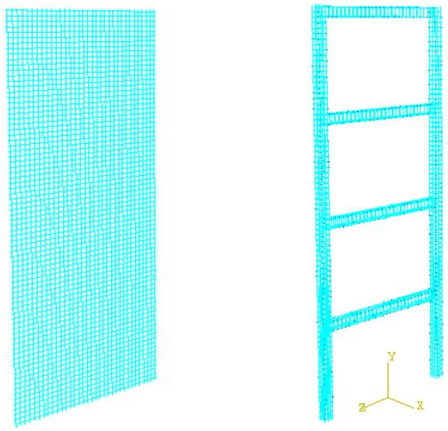

Fig.17. Rebar meshing of frame and shotcrete rebar

5.6. Model analysis and results analysis

At this stage, a job should be created so that the built model is loaded and analyzed by the software. This stage is the model processing stage. After the complete message, you can use the Result button to go to the Visualization environment and check the results of solving the problem.

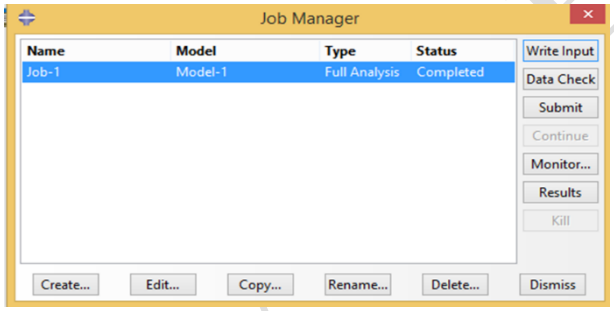

Fig. 18. Job definition for model analysis

Table 7. Values of displacement and energy input to the frame

Strengthening the model	Distance to the explosion site (m)	Amount of explosive (kg)	Maximum displacement (cm)	Entered energy (N.m)
Without retrofitting	10	100	8.7	2700
Without retrofitting	10	200	13.4	3700
Without retrofitting	10	300	17.5	4750
Without retrofitting	10	400	21	5900
Without retrofitting	20	100	1.6	980
Without retrofitting	20	200	2.1	1300
Without retrofitting	20	300	2.5	1700
Without retrofitting	20	400	2.8	2050
Reinforced	10	100	3.8	700
Reinforced	10	200	5.6	920
Reinforced	10	300	7.2	1200
Reinforced	10	400	8.6	1450
Reinforced	20	100	0.82	260
Reinforced	20	200	1	345
Reinforced	20	300	1.2	420
Reinforced	20	400	1.3	540

Table 8. Percentage increases in displacement (δ) and input energy (E_{in}) with W escalation (baseline: 100 kg TNT)

Case	Distance (m)	W Range (kg)	δ Increase (%) Unreinforced	E_in Increase (%) Unreinforced	δ Increase (%) Retrofitted	E_in Increase (%) Retrofitted
Low-Mass Escalation	10	100–200	42	27	24	32
	20	100–200	24	25	18	25
Mid-Mass Escalation	10	100–300	55	43	47	42
	20	100–300	36	42	32	38
High-Mass Escalation	10	100–400	63	54	56	52
	20	100–400	43	52	37	52

6. Conclusion

This study analyzed the blast performance of seismically designed RC observation towers, focusing on the influence of retrofitting with 5 cm shotcrete overlays on displacement and energy responses under near-field TNT explosions. The findings offer quantitative insight into the role of both explosive mass and standoff distance in governing structural demand.

Numerical simulations confirmed that shotcrete significantly enhances blast resilience by absorbing part of the incident impulse. In unretrofitted frames, increasing the TNT mass from 100 kg to 400 kg at 10 m resulted in up to 63% higher displacements and 54% more energy input. In contrast, shotcrete-retrofitted models showed 43% and 37% increases, respectively, under the same conditions, indicating a consistent 20–25% reduction in sensitivity to explosive escalation.

To generalize these results, blast response effectiveness was evaluated against the scaled distance parameter $Z = R/W^{1/3}$, which captures the combined effect of mass and distance:

- For $Z \geq 2.0$ m/kg$^{1/3}$ (moderate blast): Shotcrete reduced displacements by over 50%, and input energy by over 60% compared to unreinforced models.
- For $1.0 < Z < 2.0$ (close-in threats): Reductions ranged from 30–50%, depending on the reinforcement layout and boundary conditions.
- For $Z < 1.0$ (severe blast): Shotcrete remained effective but less dominant, with reductions of approximately 20–30%, suggesting that additional protection (e.g., barriers or energy-dissipating facades) may be required for critical applications.

Furthermore, an empirical relation was developed to estimate input energy as a function of explosive intensity:

$E_{in} \approx 0.85 \times (W/R)^{0.65} \times (1 - 0.6 \times \text{Retrofit Factor})$ ($R^2 = 0.92$ from nonlinear regression analysis)

Retrofit Factor = 1.0 (unreinforced), 0.4 (shotcrete-reinforced)

This equation facilitates preliminary sizing of protective layers and estimation of blast demand for design scenarios.

From a design standpoint, shotcrete overlays are highly recommended when $Z < 2.5$, particularly in border regions or urban infrastructures exposed to multi-hazard risks. The combined effect of seismic detailing and retrofit layering provides a dual-resilience approach. Future research is encouraged to

validate these criteria through full-scale testing, incorporate material uncertainty via probabilistic simulations, and explore advanced retrofit schemes tailored for severe blast zones.

7. Research Limitations

This study faced several limitations that may affect the precision and generalizability of the findings:

1. Lack of precise displacement data: The absence of experimental displacement measurements (e.g., laser-based tracking) constrained the ability to fully characterize the dynamic response of the structure.

2. Fixed shotcrete thickness without sensitivity analysis: The use of a constant 5 cm shotcrete layer, without conducting a ±20% sensitivity study, may result in overestimated retrofit effectiveness.

3. Simplified blast load modeling: Blast simulations were performed using CONWEP for TNT charges ranging from 100 to 400 kg at 10–20 m standoff, neglecting effects of confined or reflective explosions.

4. Limited output visualization: Failure modes and post-blast deformation images for 24 scenarios (4 TNT levels × 2 standoff distances × 3 seismic accelerations) were not included due to high computational costs (~10 hours per simulation).

5. Neglected thermal effects and brickwork simplification: Elevated temperatures exceeding 500 °C (per ASCE/SEI 59-11) were not modeled, and brick infill walls were homogenized, potentially overestimating stiffness by ~15%.

6. No progressive collapse or high strain-rate analysis: The study did not account for progressive collapse mechanisms (per GSA guidelines) or dynamic strain-rate effects exceeding $\dot{\varepsilon} > 10^3\ s^{-1}$.

7. Limitation to specific seismic intensities: The analysis focused only on seismic accelerations of 0.25 to 0.35g, without incorporating probabilistic uncertainty (e.g., Monte Carlo analysis), which may limit applicability across varying hazard zones.

8. Recommendations for Future Research

To address the above limitations and enhance the robustness of future investigations, the following directions are recommended:

1. Conduct full-scale or field tests incorporating displacement sensors to calibrate numerical models more accurately.

2. Perform sensitivity and optimization analyses for shotcrete thickness to identify performance thresholds.

3. Use hydrodynamic modeling approaches such as Smoothed Particle Hydrodynamics (SPH) to simulate complex confined or reflective blast conditions.

4. Generate comprehensive post-blast deformation visualizations via high-performance computing clusters.

5. Integrate coupled thermal–mechanical models and simulate discrete masonry behavior using Discrete Element Methods (DEM).

6. Extend analysis to include progressive collapse potential and high strain-rate material response, leveraging Split-Hopkinson Pressure Bar (SHPB) data.

7. Incorporate probabilistic Monte Carlo simulations for a broader range of seismic accelerations to improve reliability and design envelope coverage.

8. These improvements would contribute to developing more accurate, resilient, and application-specific blast-resistant design guidelines for critical infrastructure.

9. References

Akhondi, M., Ramesht, M.H., Pourrostam, T. and Golsoorat Pahlaviani, A. (2021). “Presentation of a new method for production of environment-friendly concrete using PET waste/silica fume and its

mechanical/durability properties investigation in concrete pavement", *Amirkabir Journal of Civil Engineering*, 53(3), 1107–1116. https://doi.org/10.22060/ceej.2020.16789.6346

Ashteyat, A., Shhabat, M., Alkhalaileh, A., Al-Zu'bi, M. and Abdel-Jaber, M. (2025). "Behavior of ultra-high-performance concrete under elevated temperatures: A comprehensive review of mechanical, physical, thermal, and microstructural properties", *Results in Engineering*, 26, 104960. https://doi.org/10.1016/j.rineng.2025.104960

Abebe, S. and Mohammed, T.A. (2022). "Performance assessment of reinforced concrete frame under close-in blast loading", *Advances in Civil Engineering*, 3979195, 24. https://doi.org/10.1155/2022/3979195

Aoude, H. and Li, Y. (2025). "Blast response of ultra-high performance concrete beams with high-strength steel and varying detailing levels under far-field blast loads", *Structures*, 82, 110742. https://doi.org/10.1016/j.istruc.2025.110742

Badshah, E., Naseer, A., Ashraf, M. and Ahmad, T. (2021). "Response of masonry systems against blast loading", *Defence Technology*, 17(4), 1326–1337. https://doi.org/10.1016/j.dt.2020.07.006

Barazesh, M., Shamim, I. and Anvar, S.A. (2024). "Masonry infill walls enhanced with the reinforced shotcrete in blast incidents", *Iranian Journal of Science and Technology, Transactions of Civil Engineering*, 48(4), 843–860. https://doi.org/10.1007/s40996-023-01177-9

Chen, H. Dong, Y., Tan, W., and Yuan, J. (2024). "Numerical modeling of wave interaction with a porous floating structure consisting of uniform spheres", *Physics of Fluids*, 36(8), 087133. https://doi.org/10.1063/5.0222161

Elbanna, A.M. El Sharkawy, H.M., Saleh, A.A., and Allam, N.K. (2023). "NiFeZnP nanosheets with enriched phosphorus vacancies for supercapattery electrodes", *ACS Applied Nano Materials*, 6(6), 4875–4886. https://doi.org/10.1021/acsanm.3c00606

Fan, Wu., Xu, J., Gao, H., Li, C., Xu, S., Uno, H., Xu, Y., Zhao, Y. and Shen, Z. (2021). "A cationic benzocorrole Cu(ii) complex as a highly stable antiaromatic system", *Chemical Communications*, 57(3), 383–386. https://doi.org/10.1039/D0CC06703B

Fathi, H., Lameie, T., Maleki, M. and Yazdani, R. (2017). "Simultaneous effects of fiber and glass on the mechanical properties of self-compacting concrete", *Construction and Building Materials*, 133, 443–449. https://doi.org/10.1016/j.conbuildmat.2016.12.097

Guo, S., Liu, F., Chen, J., Yang, J. and He, X. (2024). "Dynamic response and blast resistance mechanism of polyurea coating on RC slab during contact explosions", *Construction and Building Materials*, 411, 134271. https://doi.org/10.1016/j.conbuildmat.2023.134271

Gao, X., Sun, W., Zhang, W., Yuan, J., Wu, Y., Ni, W. and Feng, J. (2024). "Multi-scale study on penetration performance of steel fiber reinforced ultra-high performance concrete", *Construction and Building Materials*, 422, 135846. https://doi.org/10.1016/j.conbuildmat.2024.135846

Hao, Y. Yang, J., and Shi, J. (2025). "Machine learning-based methods for predicting the structural damage and failure mode of RC slabs under blast loading", *Buildings*, 15(8), 1221. https://doi.org/10.3390/buildings15081221

Hou, S., Li, F., Tang, H., Wen, T., Chen, Z. and Gao, H. (2022). "Investigations on the performance of shotcrete using artificial lightweight shale ceramsite as coarse aggregate", *Materials*, 15(10), 3528. https://doi.org/10.3390/ma15103528

Hosseini, S.A. and Hosseini, M. (2021). "Evaluation of the response of BFP and WFP connections under the blast loading", *Journal of Structural and Construction Engineering*, 7(Special Issue 4), 64–81. https://doi.org/10.22065/jsce.2019.148589.1661

Hemati, S.A. Derakhshan Nezhad, A.H., and Rezaifar, O. (2025). "Predicting compressive strength of heavyweight concrete using deep neural networks and Box–Behnken design", *Challenge Journal of Concrete Research Letters*, 16(4). https://doi.org/10.20528/cjcrl.2025.04.002

Jahami, A., Timsah, Y. and Khatib, J.M. (2019). "The efficiency of using CFRP as a strengthening technique for reinforced concrete beams subjected to blast loading", *International Journal of Advanced Structural Engineering*, 11(3), 411–420. https://doi.org/10.1007/s40091-019-00242-w

Karbaschi, M.B., Abbasi, A. and Yazdanian, M. (2017). "Investigating efficiency of shotcrete for retrofitting masonry buildings", *Journal of Rehabilitation in Civil Engineering*, 5(1), 47–66. https://doi.org/10.22075/jrce.2017.1147.1125

Li, L., Wu, Y., Zhao, Z., Hao, X., Xu, R., Lv, D., Huang, X., Zhao, Q., Xu, Y. and Wu, Y. (2023). "Cathode materials for calcium-ion batteries: Current status and prospects", *Chemistry – A European Journal*, 2(5), 551–573. https://doi.org/10.1002/cnl2.85

Liu, G. Yang, D., Zhang, B. (2021). "Experimental study on spall resistance of steel-fiber reinforced concrete slab subjected to explosion", *International Journal of Concrete Structures and Materials*, 15(1). https://doi.org/10.1186/s40069-021-00459-8

Luccioni, B., Isla, F., Codina, R., Ambrosini, D., Zerbino, R., Giaccio, G. and Torrijos, M.C. (2018). "Experimental and numerical analysis of blast response of high strength fiber reinforced concrete slabs", *Engineering Structures*, 175, 113–122. https://doi.org/10.1016/j.engstruct.2018.08.016

Ma, G., Li, Z., Wang, L., Wang, F. and Sanjayan, J. (2019). "Mechanical anisotropy of aligned fiber reinforced composite for extrusion-based 3D printing", *Construction and Building Materials*, 202, 770–783. https://doi.org/10.1016/j.conbuildmat.2019.01.008

Mustapha, B., Kachalla, M. and Muazu, N. (2025). "Comparative analysis of the performance of

reinforced concrete structures under blast and seismic load: A review", *International Journal of Engineering Research & Technology (IJERT)*, 14(6). https://doi.org/10.5281/zenodo.18104220

Mirzaie Aliabadi, M., Derakhshan Nezhad, A.H., Shahidzadeh, M.S. and Dadpur, A. (2025). "Date palm fibers to improve tensile strength in self-compacting concrete with silica fume", *Civil Engineering Infrastructures Journal*, 58(2), pp. 333–349. https://doi.org/10.22059/ceij.2024.368987.1988

Mirzaie Aliabadi, M. Derakhshan Nezhad, A.H., Arman, M., Feiz, D., Hemati, S.A. (2025). "The role of climate and temperature in designing regional marketing strategies for cement and plasticizers (case study: Khuzestan Province, Iran)", *Civil Engineering Infrastructures Journal*, Articles in Press. https://doi.org/10.22059/ceij.2025.384522.2177

Najimi, M. Shafei, B., Kazemian, M., Dopko, M. (2021). "State-of-the-art review of capabilities and limitations of polymer and glass fibers used for fiber-reinforced concrete", *Materials*, 14(2), 409. https://doi.org/10.3390/ma14020409

Ozturk B, Senturk T, Yilmaz C. Analytical investigation of effect of retrofit application using CFRP on seismic behavior of a monumental building at historical Cappadocia region of Turkey. *9th US & 10th Canadian Conf. on Earthquake Engineering*, 2010.

Öztürk B, Yılmaz C, Şentürk T. Effect of FRP retrofitting application on seismic behavior of a historical building at Nigde, Turkey. *14th European Conference on Earthquake Engineering*, 2010, Ohrid, Republic of Macedonia.

Pandey, A.K. and Bisht, R.S. (2016). "Numerical modelling of infilled clay brick masonry under blast loading", *Advances in Structural Engineering*, 17(4), 591–604. https://doi.org/10.1260/1369-4332.17.4.591

Ricci, P. Di Domenico, M., Verderame, G.M. (2023). "Empirical modelling of the cyclic response of reinforced concrete columns with deformed bars", *Procedia Structural Integrity*, 44, 480–487. https://doi.org/10.1016/j.prostr.2023.01.063

Salehi, P., Aghayari, R. and Fazelikelareh, M. (2025). "Behavioral analysis of reinforced concrete deep beams under dynamic loading with varying strain rates using the strut-and-tie model framework", *Civil Engineering Infrastructures Journal*, Articles in Press. https://doi.org/10.22059/ceij.2025.398909.2350

Wang, Y. (2024). "Research and development of shotcrete", *International Journal of Materials Science and Technology Studies*, 2(1), 12–18. https://doi.org/10.62051/ijmsts.v2n1.03

Xiao, S., Yang, J., Liu, Z., Yang, W. and He, J. (2024). "Effects of steel fiber content on compressive properties and constitutive relation of ultra-high performance shotcrete (UHPSC)", *Buildings*, 14(6), 1503. https://doi.org/10.3390/buildings14061503

Yang, W. Xiao, S., Yang, J., Liu, Z., He, J. (2024). "Effects of steel fiber content on compressive properties and constitutive relation of ultra-high performance shotcrete (UHPSC)", *Buildings*, 14(6), 1503. https://doi.org/10.3390/buildings14061503